THE JOURNAL OF PHYSICAL CHEMISTRY B

Article

pubs.acs.org/JPCB

Dynamics of Molecular Rotors Confined in Two Dimensions: Transition from a 2D Rotational Glass to a 2D Rotational Fluid in a Periodic Mesoporous Organosilica

Cortnie S. Vogelsberg,[1] Silvia Bracco,[2] Mario Beretta,[2] Angiolina Comotti,[2,*] Piero Sozzani,[2,*] and Miguel A. Garcia-Garibay[1,*]

[1]Department of Chemistry, University of California — Los Angeles, 607 Charles E. Young Drive East, Los Angeles, California 90095, United States

[2]Department of Materials Science, University of Milano-Bicocca, Via R. Cozzi 53, 20125 Milan, Italy

Supporting Information

ABSTRACT: The motional behavior of *p*-phenylene-d_4 rotators confined within the 2D layers of a hierarchically ordered periodic mesoporous *p*-divinylbenzenesilica has been elucidated to evaluate the effects of reduced dimensionality on the engineered dynamics of artificial molecular machines. The hybrid mesoporous material, characterized by a honeycomb lattice structure, has arrays of alternating *p*-divinylbenzene rotors and siloxane layers forming the molecularly ordered walls of the mesoscopic channels. The *p*-divinylbenzene rotors are strongly anchored between two adjacent siloxane sheets, so that the *p*-phenylene rotators are unable to experience translational diffusion and are allowed to rotate about only one fixed axis. Variable-temperature ^{2}H NMR experiments revealed that the *p*-phenylene rotators undergo an exchange process between sites related by 180° and a non-Arrhenius temperature dependence of the dynamics, with reorientational rates ranging from 10^3 to 10^8 Hz between 215 to 305 K. The regime of motion changes rapidly at about 280 K indicating the occurrence of a dynamical transition. The transition was also recognized by a steep change in the heat capacity at constant pressure. As a result of the robust lamellar architecture comprising the pore walls, the orientational dynamic disorder related to the phase transition is only realized in two dimensions within the layers, that is in the plane perpendicular to the channel axis. Thus, the aligned rotors that form the organic layers exhibit unique anisotropic dynamical properties as a result of the architecture's reduced dimensionality. The dynamical disorder restricted to two dimensions constitutes a highly mobile fluidlike rotational phase at room temperature, which upon cooling undergoes a transition to a more rigid glasslike phase. Activation energies of 5.9 and 9.5 kcal/mol respectively have been measured for the two dynamical regimes of rotation. Collectively, our investigation has led to the discovery of an orientationally disordered 2D rotational glass and its transition from rigid to soft at increasing temperature. The spectral narrowing observed in the ^{2}H NMR experiments at higher temperatures (310−420 K) is consistent with fast rotational dynamics, which remain anisotropic in nature within the robust lamellar architecture. This study suggests that exploiting reduced dimensionality in the design of solid-state artificial molecular machines and functional materials may yield access to behavior previously unrealized in 3D materials.

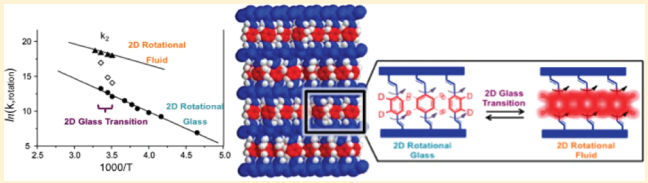

INTRODUCTION

The design of molecular rotors and related artificial molecular machines remains one of the most interesting challenges in nanotechnology.[1,2] On the basis of lessons learned from the analysis of biomolecular systems, such as skeletal muscle, ATP synthase, and others,[3] it may be expected that artificial molecular machines and functional materials based on molecular rotors should rely on assemblies that take advantage of multiple components, correlated motions, and varying degrees of periodicity, dimensionality, and symmetry.[4] Additionally, just as biomolecular machines are generally supported on membranes or in tissues, which provide a frame of reference for their motion and localize the machine where it is needed, it is also expected that artificial molecular machines should be engineered in anisotropic, highly ordered environments. As a point of entry to analyze and characterize the function of artificial molecular rotors in highly ordered self-assembling materials, we recently proposed the design and use of *amphidynamic crystals*.[5] Amphidynamic crystals are a subset of condensed phase matter with coexisting rigid and mobile molecular components that may provide a suitable platform for the development of artificial molecular machines.[6] The rigid portion of the structure makes up a solid phase, which gives shape and form to the material, constitutes the framework that supports and guides the motion of the dynamic components along predetermined degrees of freedom, and provides a well-defined frame of reference at both the molecular and macroscopic scales. Recent studies have shown that well

Received: December 11, 2011
Revised: January 5, 2012
Published: January 5, 2012

designed molecular systems are capable of forming amphidynamic solids with engineered internal motion that range from a few kilohertz to the gigahertz regime.[7]

Examples of amphidynamic materials include crystals of molecular gyroscopes[8] and compasses,[9] inclusion crystals,[10] and metal−organic frameworks,[11] as well as several coordination compounds and layered structures.[12] Studies performed on these materials have revealed that the amount of free volume and the relative flexibility of the environment proximal to the dynamic component may have a profound influence on the nature of its function and ultimately the material's bulk properties, which it constitutes.[4] Therefore, a deeper understanding of an environment's influence on engineered motion in condensed phases − namely with respect to a material's dimensionality and free volume − will result in advanced structure/function relationships to further the design of artificial molecular machines and functional materials with increasingly sophisticated behavior.

To specifically target the effects of reduced dimensionality on the dynamics of molecular rotors in amphidynamic materials, we have chosen to investigate the dynamics of *p*-phenylene rotators anchored by a rigid axle and confined within 2D layers. Platforms for such an assembly could be based on the synthesis of hierarchically ordered periodic mesoporous organosilicas (PMOs).[13] Hierarchically ordered PMOs are a class of self-assembled network-covalent solids with mesoscale pores that are built with organic ligands arranged in 2D layers via siloxane bonds. Molecular rotors have been recently studied in hierarchically ordered PMOs: the relatively low packing density of the organic elements combined with the mesoporous structure supports rapid, engineered rotation of the aromatic groups,[14,15] rendering them ideally amphidynamic. The dynamics of *p*-phenylene[14] and 4,4′-biphenylene[15] molecular rotors in such PMOs were demonstrated by variable-temperature solid-state NMR spectroscopy, which revealed fast rotational motion of the aromatic rotators and the potential to modulate their dynamics by the introduction of guests within the mesopore.[14] Other studies have shown that PMOs may be synthesized with spacers possessing tailored properties for specific functions, suggesting that the generation of hierarchically ordered PMOs with chemi- or light-responsive rotors may be possible.[16−21]

Recognizing the versatility and potential of hierarchically ordered PMO platforms and the need to further develop a correlation between 2D structures and the engineered dynamics, which they may facilitate, we analyzed the dynamics of an isotopically enriched *p*-divinylbenzene mesoporous organosilica[13d,f] (*p*-DVB-d_4 PMO) with molecular-scale periodicity using ^{2}H solid-state NMR. The use of extended organic ligands containing vinyl spacers mounted on the phenylene rotator may lead to increased degrees of freedom to facilitate rotation. Moreover, the vinyl groups provide a handle for postsynthetic modification of the PMO that could result in a useful alteration of the rotator environment.[22] This investigation has resulted in the discovery of non-Arrhenius rotational dynamics of the *p*-phenylene rotators, and the existence of a unique 2D phase transition at 280 K from which this behavior originates. The observed temperature dependence of the phenylene rotational frequency in *p*-DVB-d_4 PMO reflects changes in the structure from a relatively rigid rotator environment to one that is highly fluid within a narrow temperature range, where the siloxane scaffold maintains the alignment of the rotors in robust 2D amphidynamic arrays. Above the transition, these arrays become 2D fluidlike nanophases organized within the covalent architecture. The pervasiveness of the motion extended to the entire confined organic phase is also unusual because it occurs in a material showing both a high surface area and stability to very high temperatures. This finding is particularly relevant in the design of amphidynamic materials because molecular motion in organized arrays confined to reduced dimensionalities can be harnessed to develop materials with intriguing properties such as ferroelectricity.

EXPERIMENTAL SECTION

Synthesis. Samples of the *p*-DVB-d_4 PMO were prepared as described previously via the solvothermal method using *p*-bis[(*E*)-2-(triethoxylsilyl)vinyl]benzene-d_4 and octadecyl trimethylammoniumbromide surfactant under alkaline conditions.[13d] The deuterium-enriched silsesquioxane ligand was obtained via a Heck coupling reaction between commercially available *p*-dibromobenzene-d_4 and triethoxy(vinyl)silane.[23] The sample of the *p*-DVB-d_4 PMO was obtained by mixing the components at 25 °C followed by heating to 95 °C for 22 h. The excess surfactant was removed by stirring the resulting suspension in acidic ethanol for 6 h at 55 °C. The natural abundance *p*-DVB PMO, constituted by C−H aromatic units, was prepared following the above procedure starting from *p*-bis[(*E*)-2-(triethoxylsilyl)vinyl]benzene.

Solid-State NMR Spectroscopy. Solid-state ^{2}H NMR spectroscopy experiments were performed on a Bruker 300 Avance spectrometer operating at a frequency of 46.07 MHz under a static magnetic field of 7.04 T, using a Bruker 4 mm wide-line probe. Fully relaxed spectra (15 s recycle delay) were acquired with the quadrupolar spin−echo pulse sequence, $(\pi/2)x - t_1 - (\pi/2)y - t_2$, with a $\pi/2$ pulse of 2.1 μs and a pulse spacing of $t_1 = t_2 = 50$ μs. Spectra obtained with a pulse spacing between 30 and 70 μs had the same line shapes. The stability and accuracy of the temperature controller (Bruker B-VT2000) were approximately 1 K. Theoretical simulation of ^{2}H NMR spectra for a two-site 180° jump model was performed by the program Express 1.0,[24] with a quadrupolar coupling constant of 180 kHz and an asymmetry parameter of $\eta = 0.02$. The simulations are obtained for a log-Gaussian distribution of jump rates by superposition of 61 spectra for different jump rates. A single distribution width of $\sigma = 1.25$ was used. ^{13}C MAS NMR measurements were performed on a Bruker Avance 300 instrument operating at 7.04 T. Ramped-amplitude cross-polarization experiments were performed at a spinning speed of 15 kHz using a recycle delay of 10 s and a contact time of 0.05 and 2 ms. The $\pi/2$ pulse used for proton was 2.9 μs.

X-ray Powder Diffraction. X-ray powder diffraction patterns were measured on a θ/θ D8-Advance powder diffractometer (Bruker) using Cu Kα_1 radiation at 40 kV and 40 mA (Bragg−Brentano geometry). The X-ray powder diffraction patterns were recorded with a scanning speed of 0.2° 2θ/min.

Adsorption Measurements. Nitrogen adsorption−desorption isotherms were measured at liquid nitrogen temperature using a Micromeritics ASAP 2050 analyzer. The samples were outgassed overnight at 160 °C under vacuum. Surface area was calculated using the Brunauer, Emmet, and Teller (BET) model. The pore-size distributions were evaluated following the method developed by Barret, Joyner, and Halenda (BJH model) for cylindrical pores with Kruk−Jaroniec−Sayari correction and by nonlinear DFT analysis.

dx.doi.org/10.1021/jp2119263 | J. Phys. Chem. B 2012, 116, 1623−1632

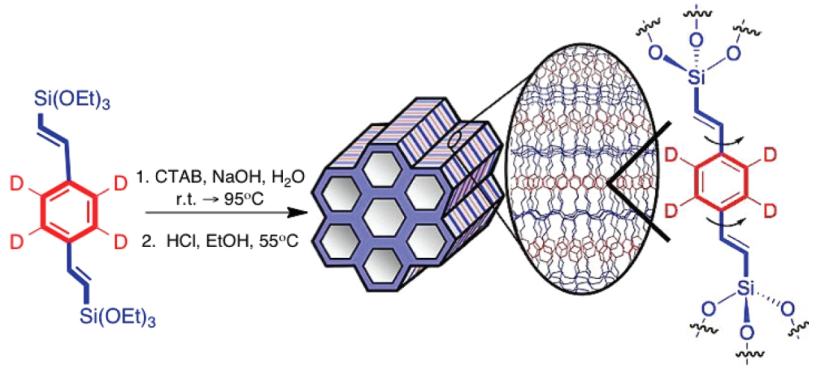

Figure 1. Solvothermal synthesis and schematic representation of *p*-DVB-d_4 PMO with molecularly ordered walls. Red represents the dynamic phenylene-d_4 moiety, and blue represents the *p*-vinyl groups and siloxane layers considered static relative to the rotating component. As indicated by the color code, the long axes of the *p*-DVB-d_4 units are parallel to long axes of the channels.

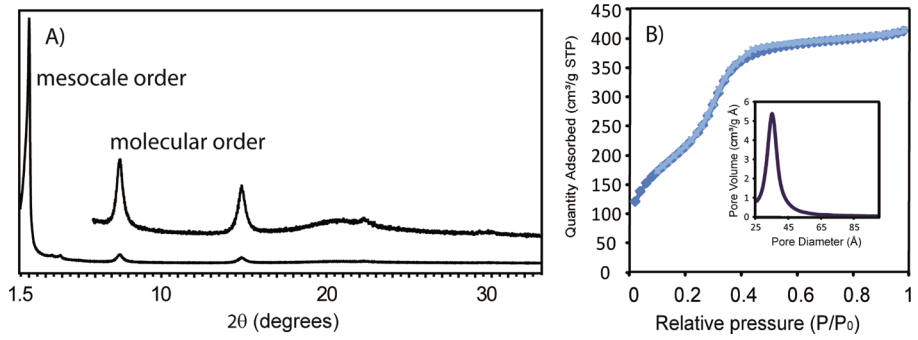

Figure 2. A) Powder X-ray diffraction pattern and B) N_2 adsorption isotherm at 77 K of the *p*-DVB-d_4 PMO sample. The pore distribution analysis using BJH method is reported in the insert.

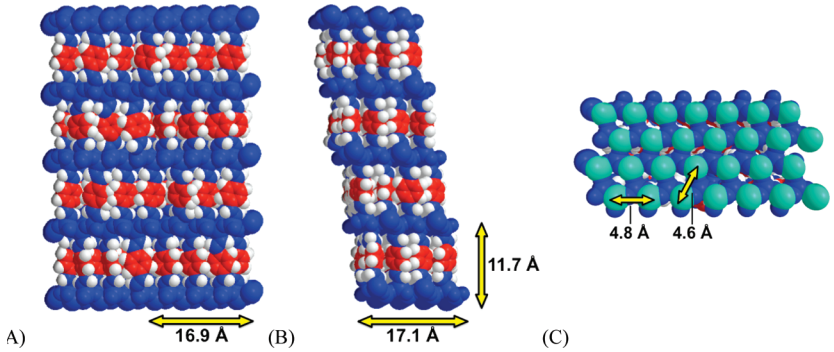

Figure 3. Idealized model of a molecularly ordered *p*-DVB-d_4 PMO pore wall fragment represented with a spacefilling model. The perspectives shown are of (A) the pore wall fragment and (B) a cross-section of the wall, with dynamic phenylene rotators depicted in red and the (relatively) static divinyl groups and siloxane layers shown in blue. (C) Bird's eye view of a siloxane layer fragment illustrating the proximity of neighboring rotator axles, with anchoring silicon atoms depicted in teal.

Thermal Analyses. Differential scanning calorimetry (DSC) traces were performed on a Mettler Toledo Thermal Analysis System equipped with a nitrogen low-temperature apparatus. The experiments were run under nitrogen atmosphere in an open Al-crucible. The samples were first heated to 160 at 10 °C/min, then, after cooling, the DSC runs were carried out from −150 to 200 °C at distinct rates of 10 °C/min and 5 °C/min. The sample weights for the DSC measurements were on average approximately 5 mg, and were measured to an accuracy of 0.05 mg. The stability of the sample was evaluated using a PerkinElmer TGA-7 instrument. About 10 mg of sample was heated from 25 to 700 °C at a heating rate of 10 °C/min under nitrogen.

RESULTS AND DISCUSSION

The synthesis of hybrid *p*-DVB-d_4 periodic mesoporous organosilica derived from *p*-bis[(*E*)-2-(triethoxylsilyl)vinyl]-benzene-d_4 containing deuterated *p*-phenylene rings is schematically depicted in Figure 1. The ordered arrangement of the structure, on both the mesoscale and the nanoscale, was shown by the X-ray powder diffraction pattern, which displayed a sharp peak in the small-angle scattering region with a *d*-spacing of 46.3 Å and two minor peaks with a *d*-spacing of 26.5 and 23.1 Å, corresponding to the 2D hexagonally ordered (*p6mm*) mesopore arrangement with a lattice constant of 53.5 Å (Figure 2). Additional peaks in the high-angle scattering region with *d*-spacings of 11.8, 6.0, 4.0, and 3.0 Å confirmed the

dx.doi.org/10.1021/jp2119263 | J. Phys. Chem. B 2012, 116, 1623−1632

presence of lamellar ordering of the organic moieties within the pore walls.[13b,d,f] Nitrogen physisorption analysis revealed a type-IV isotherm corresponding to uniform mesopores with a Brunauer–Emmett–Teller (BET) specific surface area of 798 m^2/g, a pore diameter of 35.2 Å (BJH) or 36.0 Å (DFT) and a mesopore volume of 0.70 cm^3/g.

Details of the structure at the molecular level may be provided by considering an idealized pore wall fragment model based on the powder X-ray diffraction data and the adsorption measurements (Figure 3). The model is consistent with the one obtained by Cornelius et al.[13f] and akin to the structure proposed by Inagaki et al. for the molecularly ordered *p*-phenylene periodic mesoporous organosilica.[13c] As shown in parts A and B of Figure 3, the pore walls consist of axially substituted *p*-divinylbenzene-d_4 ligands arranged in layers with the molecular long axis parallel to the channel direction and anchored at each end by a siloxane network. The siloxane network is comprised of six-membered siloxane [cyclo-$(SiO)_6$] rings with the divinylbenzene ligands adopting axial positions above and below each layered plane. The closest distance imposed by the model structure between neighboring phenylene axes is 4.6 Å (part C of Figure 3), which is in good agreement with the broad signal centered at 4.4 Å in the PXRD pattern. Whereas this distance is greater than the van der Waals contact of 3.4 Å for two face-to-face parallel *p*-phenylenes, each rotator has a revolution radius of ca. 3 Å (including van der Waals surface) and a minimum lateral encumbrance of 1.7 Å due to the π-electron clouds of the neighboring aromatic ring. Therefore, an unhindered 180° flip rotation requires the distance between adjacent axes of the *p*-phenylene moieties to be greater than 4.7 Å. As a consequence of this, the organization in the PMO walls cannot satisfy a close packing arrangement and may generate disorder of the rotators within the 2D layers, as depicted in parts A and B of Figure 3. This arrangement should also have interesting effects on the dynamics of the rotators.

The number of *p*-DVB-d_4 rotators within the wall was estimated by considering the wall thickness and the molecular distances from the structural model. The pore wall thickness, b_d, can be obtained from the equation $b_d = (2/\sqrt{3})\, d_{100} - w_d$, where d_{100} is the PXRD (100) interplanar spacing and w_d the pore diameter.[13c] With a calculated thickness of the pore wall b_d = 18.3 Å (using the BJH pore diameter) or b_d = 17.5 Å (using the DFT model pore diameter), one can estimate that the wall thickness comprises ca. 4 molecules as illustrated in part B of Figure 3. In addition to the limited size of the orientationally ordered rotator domains, the different local environments and rotational potentials inside the wall and at the interface may have an effect on the local order and rigidity, and a large impact on the rotational dynamics. The thin pore walls expose a large fraction of phenylene rotators to the interface of the mesopore, reducing the number of neighboring phenylene rotators. Recent studies on small molecules and polymers confined to such restricted dimensions, including thin films,[25] self-assembled monolayers,[26] molecular cages and containers,[2e,27] and confined porous structures[25a,28] have revealed significant deviations from bulk-phase behavior with respect to phase transitions, morphology, and chemical reactivity. It has been suggested that interfacial effects, changes in the available degrees of freedom, and changes in entropy resulting from nanoscale confinement induce these deviations.[29] In the case of the *p*-DVB-d_4 PMO, the confining parameters are the thickness of the pore walls, the size of orientationally ordered rotator domains within the 2D layers, and the positional anchoring of the *p*-DVB-d_4 axes imposed by the siloxane layer.

Rotator Dynamics by Solid-State NMR Spectroscopy. The solid-state ^{13}C CP/MAS NMR spectrum of the isotopically enriched *p*-DVB-d_4 PMO recorded with a contact time of 2 ms showed the presence of four signals (part A of Figure 4) for the

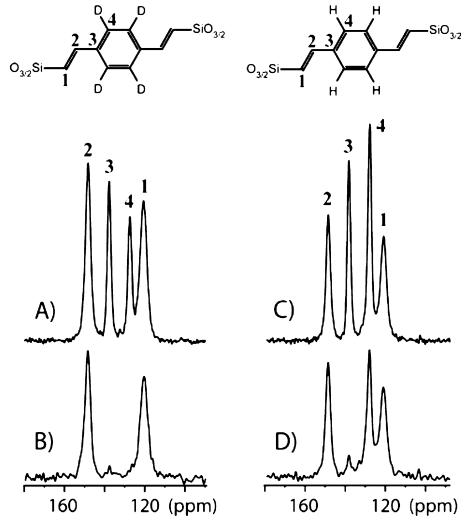

Figure 4. ^{13}C CP/MAS NMR spectra of *p*-DVB-d_4 PMO and natural abundance *p*-DVB PMO with 2 ms (A and C) and 50 μs (B and D) contact times, respectively.

aromatic and vinyl carbons in agreement with the symmetry of the divinylbenzene organic moiety within the framework, as depicted in the model structure (part A of Figure 3). A direct demonstration of the substitution of hydrogens with deuterons on the aromatic ring was provided by a ^{13}C CP/MAS spectrum with a contact time as short as 50 μs, which exhibits only two signals due to the vinyl carbons covalently bonded to hydrogens (part B of Figure 4). The resonance of deuterated C(4)^{2}H aromatic carbons at δ_C = 127.1 ppm is fully suppressed, because the aromatic carbons are not near a hydrogen source of magnetization.[30] For comparison, the spectrum of the natural abundance *p*-divinylbenzene sample (*p*-DVB PMO) with a short contact time clearly shows the signal of the C(4)H aromatic moiety (part D of Figure 4). With such a short contact time, the aromatic C(3) signal at δ_C = 137.6 ppm is also suppressed because the C(3) carbon does not bear covalently bonded hydrogens. The spectrum of the *p*-DVB PMO at longer contact times (part C of Figure 4) displays the narrowest line width for the signal of C(4)H aromatic carbons, which is a first indication of fast dynamics of the *p*-phenylene rotators in the framework. Indeed, the ^{13}C spin-lattice T_1 relaxation times, which are related to the motional behavior of the ^{13}C nuclei, exhibit at room temperature a value as short as 600 ms for C(4)H aromatic carbons, consistent with fast molecular motion of the *p*-phenylene rotators about their axis of rotation. The very short ^{13}C relaxation time is indicative of an efficient relaxation mechanism that occurs when the motional frequency matches the observation frequency, which is 75 MHz in the present case. On the contrary, the C(3) carbon shows longer ^{13}C relaxation times of 8 s because it sits on the axis of molecular rotation and its motion is restricted.

The rate and trajectory of the phenylene rotational dynamics in the isotopically enriched *p*-DVB-d_4 PMO were analyzed by variable-temperature solid-state ^2H NMR spectroscopy.[31] This

dx.doi.org/10.1021/jp2119263 | J. Phys. Chem. B 2012, 116, 1623–1632

method relies on the high sensitivity of the quadrupolar interaction between the nuclear spin and the electric field gradient at the nucleus, which depends strongly on the orientation of the C−^{2}H bond vector with respect to the direction of the external magnetic field. Powdered samples with static deuterons are characterized by a broad symmetric spectrum known as a Pake pattern that consists of two singularities and two outer shoulders separated by ca. 135 and 270 kHz respectively for aromatic C−^{2}H bonds.[32] In contrast, deuterons experiencing dynamic processes in the range of 10^4 to 10^8 Hz display spectral changes that depend both on their frequencies and trajectories of motion. For the current study, we take advantage of the well-characterized spectral changes that occur when phenylene groups rotate about their 1,4-axis, which in most cases involves discrete jumps given by an angular displacement of 180°, also known as a 2-fold ring flip.[33]

Measurements with *p*-DVB-d_4 PMO were carried out using a quadrupolar spin−echo pulse sequence at 17 different temperatures from 215 to 420 K, and the experimental line shapes were compared with simulations carried out with the program Express 1.0 (Figure 5). The spectrum measured at 215 K was a

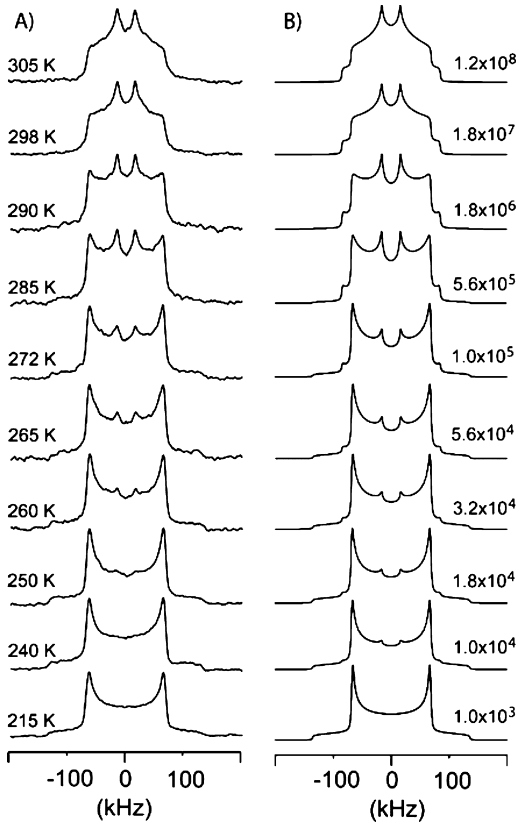

Figure 5. A) Variable-temperature ^{2}H solid-state NMR spectra from 215 to 305 K of *p*-DVB-d_4 PMO and B) line shape analysis and calculated rates k_I (Hz) of rotation of *p*-phenylene moieties. The k_I rates were determined from ^{2}H NMR line shape analysis considering a single component log-Gaussian distribution.

characteristic Pake pattern, suggesting motion in the slow exchange regime (10^3 Hz), with a typical quadrupolar coupling constant QCC = 180 kHz and a small asymmetry parameter η = 0.02. The spectra measured between 215 and 305 K were initially simulated with a model that considers 2-fold ring flips in the intermediate exchange regime with frequencies (k_I) that range from ca. 10 kHz at the lower temperature up to 120 MHz at 305 K. The simulations required a log-Gaussian distribution of jump rates with a width of σ = 1.25, suggesting the presence of a motional frequency distribution arising from the presence of rotator disorder within the 2D layers.[34] Heterogeneous dynamics are characteristic of amorphous solids and glassy polymers and define a certain length scale in which molecular rearrangements are influenced by a specific environment. Therefore, the log-Gaussian distribution of jump rates in this study suggests that the dynamics of the *p*-phenylene rotators within the walls also undergo some dynamic heterogeneity, the result of variances among different orientationally ordered rotator domains.[35] It is interesting to note that additional degrees of freedom brought about by the divinyl substituents to the phenylene rings do not result in additional trajectories of motion within the 215−305 K temperature range. This observation is consistent with the model structure, which has the two double bonds in the trans configuration with their points of anchorage away from a coaxial alignment and unable to provide a rotational axle to the entire moiety.

To determine the activation energy, E_a, of rotation and the pre-exponential factor, k_0, the natural logarithm of the calculated frequencies for phenylene rotation, ln(k_I), and the corresponding inverse temperatures were used to construct an Arrhenius plot (part A of Figure 6). Deviations from linearity

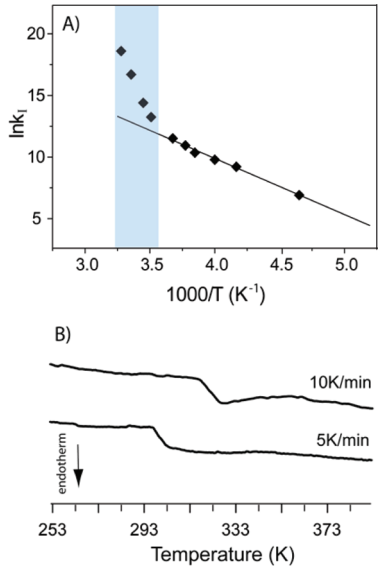

Figure 6. Arrhenius plot of A) ln(k_I) vs temperature in the 215−305 K range. The k_I rates were determined from ^{2}H NMR line shape analysis. In the 215−272 K range, a linear least-squares regression fit of r^2 = 0.99 is obtained. B) Calorimetric runs of *p*-DVB-d_4 PMO at two heating rates.

become apparent from the reported data, and non-Arrhenius behavior is evident in the plot. In particular, a dramatic increase of the k_I frequencies is observed within a narrow range of temperatures (highlighted in blue). As a consequence, the apparent activation energy E_a depends upon the temperature range chosen for a linear fit of the Arrhenius equation (ln k_I = ln k_0 − E_a/RT), giving rise to the calculation of an unreasonably large activation energy and pre-exponential value in the high temperature limit and pre-exponential values. However, in the low temperature region (215−272 K), a linear behavior can be recognized that, after fitting to the Arrhenius

dx.doi.org/10.1021/jp2119263 | J. Phys. Chem. B 2012, 116, 1623−1632

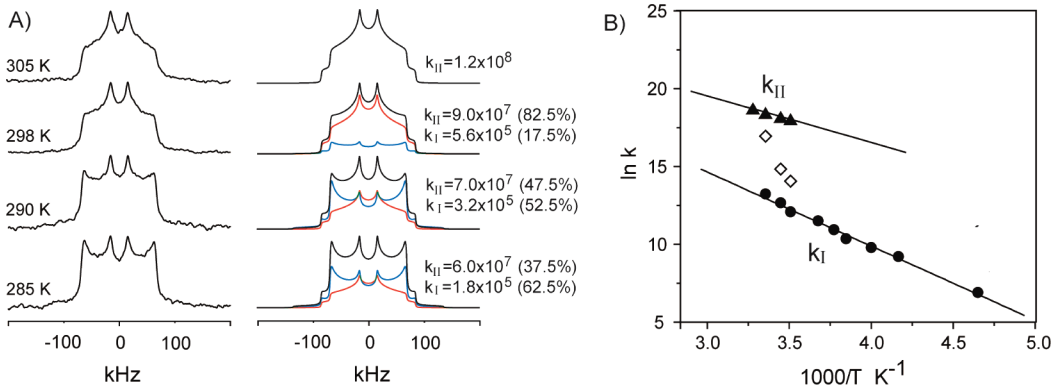

Figure 7. A) Experimental and simulated ^{2}H NMR spectra in 285−305 K range. The spectra were simulated as the sum of two profiles weighted by the fraction of the two components. B) Arrhenius plots of both the low-frequency k_I (full circle) and high-frequency k_{II} components (full triangle). The open diamonds represent the frequency obtained as the sum of the rates of the two components weighted by their fraction.

equation, corresponds to an E_a = 9.1 kcal/mol and a $k_0 = 1.7 \times 10^{12}$ Hz. These values are consistent with those reported in the literature for the activation energy of a 180° flip of phenylenes in crystalline materials[8,10] and polymers[36] and the pre-exponential factor of an individual *p*-phenylene rotator, respectively. Notably, the pre-exponential factor reflects the highest rotational frequency for a hypothetical phenylene rotator with no steric barriers. For an elementary *p*-phenylene rotator in the gas phase, transition state theory suggests that the pre-exponential factor is related to the frequency of oscillation at the bottom of the potential well, which for low-frequency torsional modes is of the order of ca. 10^{12} Hz.[37] From an alternative perspective, the pre-exponential factor may be taken as the limit of rotational inertia for a hypothetical rotator with no intrinsic (steric and electronic) barriers. In the case of a *p*-phenylene, this value has been estimated to be 2.4×10^{12} Hz,[4,5,38] which is close to the experimental value measured in this temperature range and for phenylene rotators in several other systems.

In contrast to the measurements between 215−272 K, Arrhenius analysis of the data acquired at higher temperatures in the range of 272 to 305 K results in the calculation of unreasonably large values of both the activation energy and the pre-exponential factor for a *p*-phenylene rotator (i.e., apparent values of ca. 47 kcal/mol and 4.0×10^{41} Hz, respectively). Such unusually large values with corresponding strongly curved Arrhenius plots characterized by a tangent that increases as a function of temperature have been documented for rotational motion in bulk glasses and indicate the presence of a transition to a system possessing more rapid dynamics.[29] For thermally activated processes near a glass transition region, the apparent pre-exponential factor and activation energy are unusually large.[39]

In search of direct evidence for a transition, the calorimetric behavior of *p*-DVB-d_4 PMO as a function of temperature was investigated. Indeed, the calorimetric scans at variable heating rates of 10 and 5 °C/min showed the occurrence of a localized increase in heat capacity (C_p) at 320 and 300 K at constant pressure, respectively (part B of Figure 6). The transition temperature decreases rapidly with diminishing heating rate, leading to an extrapolated transition temperature of 280 K for the limit of zero heating rate. The transition's dependence on the scanning rate is typical of a kinetic phenomenon, reminiscent of a glass transition. The larger heat capacity above the transition may be correlated to the onset of additional degrees of freedom gained by the rotators in their ensemble. Below the transition, a decrease in heat capacity at low temperature can be associated with the larger influence of intermolecular interactions.

As a consequence, the ^{2}H NMR spectra acquired immediately above the transition could be reinterpreted by introducing a second fast-rate component (k_{II}), which adds to the low-rate component (k_I) to account for the sudden onset of higher frequency rotation (part A of Figure 7). This line shape analysis is consistent with a previous study regarding the ^{2}H NMR spectral characterization of phenylene rotation in the mesogenic side chains of a liquid-crystalline polymer near its glass transition, which displayed contributions from motion in both the rapid and slow exchange limits.[35a] In the PMO, the second fast-rate component exhibits rates as high as 10^8 Hz, and its contribution to the total profile appears to increase drastically from 37.5% to 82.5% in a restricted temperature range between 285 to 298 K. The k_{II} component may result from the progressive softening of the rotator environment from a glasslike to a fluidlike rotator nanophase confined within the layers. Using a model that identifies two distinct components in the total dynamic behavior allows for the construction of simulated ^{2}H NMR profiles, which are in excellent agreement with the experimental spectra and whose Arrhenius plots yield values realistic for both the pre-exponential factor and the activation energy. Indeed, the low and high frequency components, when plotted in the ln *k* versus $1/T$ chart (part B of Figure 7), generate excellent linear regression coefficients of $r^2 = 0.99$ with physically reasonable activation energies of 9.5 and 5.9 kcal/mol respectively, whereas the pre-exponential factors of both are coincident with the expected $k_0 \approx 10^{12}$ Hz for a *p*-phenylene rotator.

It should be noted that the E_a for the slower component associated with the more rigid glassy state is two times that of the ca. 4.7 kcal/mol calculated gas-phase barrier for phenylene rotation in *p*-divinylbenzene (Supporting Information)[40,41] suggesting that steric hindrance has a large influence on *p*-phenylene rotation in the lamellar phase at lower temperatures.[42] A hindered environment is consistent with a distance of ~4.4 Å between the axes of adjacent rotators, which is less than the 4.7 Å distance estimated for unhindered 180° flips (vide supra) and smaller than the well-known 5.85 Å kinetic diameter for benzene and *p*-xylene.[43] Instead, at temperatures above the transition, the activation energy of the high frequency dynamic component is only ca. 5.9 kcal/mol − much closer to

dx.doi.org/10.1021/jp2119263 | J. Phys. Chem. B 2012, 116, 1623−1632

the intrinsic gas-phase electronic barrier for phenylene rotation in *p*-divinylbenzene. Such a low rotational barrier may be facilitated by wobbling and/or librations, which would result in additional degrees of freedom leading to a highly flexible, fluidlike local environment for the rotators.[42] Actually, by an additional temperature increase from 310 to 420 K, narrowing spectral profiles with weaker shoulders, which deviate from the 180° jump model become apparent (Figure 8). This result

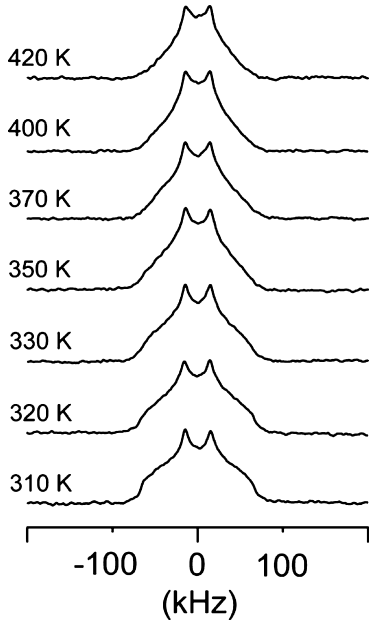

Figure 8. Variable-temperature ^{2}H solid-state NMR spectra from 298 to 420 K. The 180° flip mechanism is in the fast exchange limit and deviates from a two-site jump model.

suggests that the *p*-phenylene groups undergo large amplitude librations and/or that they are able to explore additional trajectories including wobbling. It is also worthwhile to note that the ^{2}H NMR line shapes do not collapse to a single isotropic line indicating that the *p*-phenylene moieties preserve their anisotropic motion even at the highest temperatures analyzed. The robust framework provides fixed pivots to the molecular rotors aligned in the channel walls and the uniaxial orientation of the *p*-phenylene rotators is substantially maintained during their rotational dynamics over the entire temperature range investigated.

Transition from a 2D Rotational Glass to a 2D Rotational Fluid. The temperature dependence of *p*-phenylene rotation in the investigated PMO is associated with a change in heat capacity related to the onset of additional degrees of freedom, which typically occurs among organic materials, especially in the amorphous phase of polymers. Some *p*-phenylene containing polymers, such as polycarbonate and polyvinylenephenylene,[44] exhibit fast motion of the phenylene rings below their glass transition that is characterized by single 180° flip rotations with activation energies of about 8−10 kcal/mol. This is comparable to the 180° flip rotations, E_a = 9.5 kcal/mol, that the PMO rotators undergo in the low temperature phase. Therefore, at low temperatures the dynamics of *p*-phenylene rotators confined in the 2D layers of the PMO are consistent with rotation in a glasslike state while at increasing temperatures above the transition, motional domains grow statistically within the PMO pore wall layers generating 2D fluidlike nanophases. For organic and inorganic glasses in general, the transition from a glassy state into a viscous isotropic fluid by increasing temperature has been well documented,[45] although in the PMO the molecular rotors maintain their anisotropic alignment within the molecular layer. In fact, in the PMO under investigation, orientational dynamic disorder is only allowed in the plane perpendicular to the channel axis and the organic layers exhibit anisotropic dynamical properties through the alignment of the *p*-DVB axes. The dynamical disorder restricted to two dimensions and manifested in the rotator dynamics defines a 2D fluidlike rotator phase at room temperature, which, on cooling, undergoes a transition to a 2D glasslike rotator system accompanied by a heat capacity change (Figure 9). In spite of the increased fluidity, at high temperature the covalent framework of PMOs holds the whole architecture into register, whereas in conventional molecular materials the molecules and polymer chains collectively gain enough freedom to collapse to a low-viscosity isotropic state.

A further analogy to the investigated PMO behavior is with thermotropic liquid-crystalline materials,[46] which can undergo calorimetric transitions with temperature that are associated with increased degrees of motion without complete isotropic reorientation of the molecules. In particular, studies with liquid-crystalline polymers have shown that phase and glass transitions

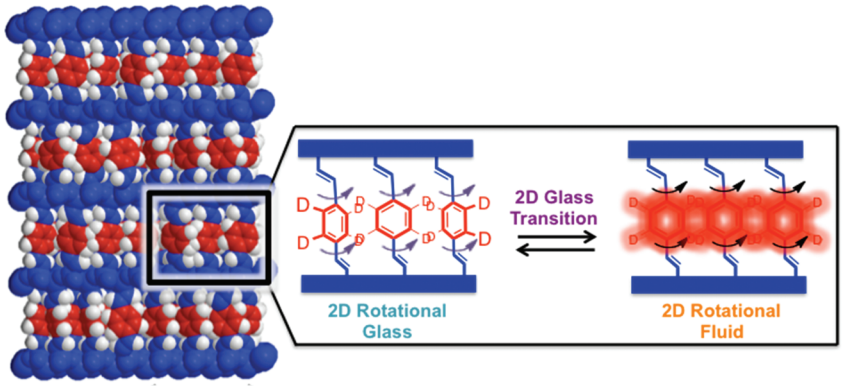

Figure 9. Dynamical disorder restricted to two dimensions is manifested in the rotator dynamics. A 2D fluidlike rotator phase exists at room temperature with rapid rotational dynamics. Upon cooling, the material undergoes a transition to a 2D glasslike rotator system accompanied by a heat capacity change and the rotator dynamics heterogeneously slow down by orders of magnitude.

dx.doi.org/10.1021/jp2119263 | *J. Phys. Chem. B* 2012, 116, 1623−1632

have a significant impact on the rotational dynamics of phenylene moieties contained in the mesogenic side groups.[35] Below the glass transition, liquid-crystalline order is maintained in a glassy state, with features that may be similar to the oriented 2D rotational glass composing the PMO pore walls. However, the anisotropic nature of liquid-crystalline materials persists only in limited temperature ranges, and at increasingly higher temperatures the mobile moieties eventually reach an isotropic state with fully incoherent molecular motion. In stark contrast to liquid crystalline materials, the PMO covalent siloxane scaffold prevents translational movement and melting of the framework over hundreds of degrees, up to the decomposition temperature of more than 500 °C, yet, it displays a remarkable 2D transition of the phenylene rotators confined within the robust layers!

Exploiting the dynamic behavior observed for the *p*-phenylene rotators, above and below their transition, represents a useful means to elicit a very large and significant thermal response within a narrow temperature range. The *p*-phenylene rotators in the PMO undergo engineered, anisotropic rotation characterized by a low-frequency component, which can be drastically increased to undergo high frequency rotation within fluid, anisotropic 2D nanophases near room temperature. Interestingly, similar non-Arrhenius behavior has been documented in anisotropic biological assemblies, such as proteins and membranes.[47] Such dynamic behavior is integral to biomolecular function, as the biochemical activity in these assemblies directly correlates with the onset of certain motions.[48]

CONCLUSIONS

In this study, an isotopically enriched *p*-divinylbenzene mesoporous organosilica with molecular-scale periodicity was probed using variable-temperature ^{2}H spin-echo solid-state NMR spectroscopy to investigate the effect of temperature on the rotational dynamics of *p*-phenylene moieties confined in a 2D nanolayer. Unexpectedly, a straightforward Arrhenius-type model could not explain the dynamical behavior of the phenylene moieties. Instead, a sharp motional change combined with a heat capacity jump and a dramatic, temperature-based increase in rotational freedom of the rotators was discovered. It is postulated that the system undergoes a change in dynamics from a relatively rigid to a fluidlike medium. This is a remarkable result for an orientational 2D material containing layers of aligned rotators with only one degree of rotational freedom and no translational freedom. We suggest that such behavior might be a general phenomenon in *p*-phenylene PMOs with molecular-scale order, and this study provides insight on how to better exploit their properties in the development of amphidynamic materials.

The realization of collective mobility and fluidity in a crystallike environment suggests that PMOs containing functionalized *p*-phenylene rotators should be exciting candidates for the development of artificial molecular machines and functional materials. The discovery of a transition within a 2D anisotropic environment gives general insight on how to design anisotropic, stimuli-responsive bulk materials whose engineered dynamical properties vary widely over very narrow temperature ranges. For PMOs in specific, the presence of porosity and the easy accessibility of the rotators to external agents (from gas or liquid phases) constitute an additional way to tune their properties, strengthening their usefulness in the design of artificial molecular machines and materials.

ASSOCIATED CONTENT

Supporting Information

Details on the synthesis of the ligand and the PMO, ^{1}H and ^{13}C NMR spectra of the *p*-DVB-d_4 ligand in $CDCl_3$, PXRD pattern and nitrogen adsorption isotherm of the natural abundance *p*-DVB PMO, and details regarding the ab initio calculation of the barrier to rotation of *p*-divinylbenzene, including the complete ref 40. This material is available free of charge via the Internet at http://pubs.acs.org.

AUTHOR INFORMATION

Corresponding Authors

*E-mail: angiolina.comotti@mater.unimib.it (A.C.).
*piero.sozzani@mater.unimib.it (P.S.).
*mgg@chem.ucla.edu (M.A.G.-G.).

ACKNOWLEDGMENTS

Work at UCLA was supported by grants NSF DMR0605688 and creativity extension DMR0937243. C.S.V. acknowledges support from NSF: IGERT MCTP grant DGE0114443. Cariplo Foundation and Regione Lombardia are acknowledged for the financial support. We thank Dr. Fernando Uribe-Romo and Bernardo Moltrasio for assistance with the *p*-DVB PMO model and nitrogen physisorption, respectively.

REFERENCES

(1) (a) Kay, E. R.; Leigh, D. A.; Zerbetto, F. *Angew. Chem., Int. Ed.* **2007**, *46*, 72−191. (b) Skopek, K.; Hershberger, M. C.; Gladysz, J. A. *Coord. Chem. Rev.* **2007**, *251*, 1723−1733. (c) Browne, W. R.; Feringa, B. L. *Nature Nanotechnol.* **2006**, *1*, 25−35. (d) Kottas, G. S.; Clarke, L. I.; Horinek, D.; Michl, J. *Chem. Rev.* **2005**, *105*, 1281−1376.

(2) (a) van Delden, R. A.; Wiel, M. K. J.; Pollard, M. M.; Vicario, J.; Koumura, N.; Feringa, B. L. *Nature* **2005**, *437*, 1337−1340. (b) Horinek, D.; Michl, J. *Proc. Natl. Acad. Sci.* **2005**, *102*, 14175−14180. (c) Skopek, K.; Gladysz, J. A. J. *Organomet. Chem.* **2008**, *693*, 857−866. (d) Karim, A. R.; Linden, A.; Baldridge, K. K.; Siegel, J. S. *Chem. Sci.* **2010**, *1*, 102−110. (e) Scarso, A.; Onagi, H.; Rebek, J. Jr. *J. Am. Chem. Soc.* **2004**, *126*, 12728−12729. (f) Leigh, D. A.; Wong, J. K. Y.; Dehez, F.; Zerbetto, F. *Nature* **2003**, *424*, 174−179. (g) Pease, A. R.; Jeppesen, J. O.; Stoddart, J. F.; Luo, Y.; Collier, C. O.; Heath, J. R. *Acc. Chem. Res.* **2001**, *34*, 433−444. (h) Jian, H.; Tour, J. M. *J. Org. Chem.* **2003**, *68*, 5091−5103. (i) Akutagawa, T.; Shitagami, K.; Nishihara, S.; Takeda, S.; Hasegawa, T.; Nakamura, T.; Hosokoshi, Y.; Inoue, K.; Ikeuchi, S.; Miyazaki, Y.; et al. *J. Am. Chem. Soc.* **2005**, *127*, 4397−4402.

(3) (a) Kinbara, K.; Aida, T. *Chem. Rev.* **2005**, *105*, 1377−1400. (b) Atsumi, T.; McCarter, L.; Imae, Y. *Nature* **1992**, *395*, 182−184. (c) Boyer, P. D. *Annu. Rev. Biochem.* **1997**, *66*, 717−749.

(4) Vogelsberg, C. S.; Garcia-Garibay, M. A. *Chem. Soc. Rev.* **2012**, Advance Article. DOI: 10.1039/C1CS15197E.

(5) Khuong, T. V.; Nunez, J. E.; Godinez, C. E.; Garcia-Garibay, M. A. *Acc. Chem. Res.* **2006**, *39*, 413−422.

(6) (a) Garcia-Garibay, M. A. *Proc. Natl. Acad. Sci.. U.S.A.* **2005**, *102*, 10793−10796. (b) Garcia-Garibay, M. A. *Nat. Mater.* **2008**, *7*, 431−432.

(7) (a) Karlen, S. D.; Garcia-Garibay, M. A. *Top. Curr. Chem.* **2006**, *262*, 179−228. (b) Garcia-Garibay, M. A. *Angew Chem. Int. Ed.* **2007**, *46*, 8945−8947.

(8) (a) Dominguez, Z.; Dang, H.; Strouse, M. J.; Garcia-Garibay, M. A. *J. Am. Chem. Soc.* **2002**, *124*, 2398−2399. (b) Khuong, T. V.; Zepeda, G.; Ruiz, R.; Khan, S. I.; Garcia-Garibay, M. A. *Cryst. Growth Des.* **2004**, *4*, 15−18. (c) Godinez, C. E.; Zepeda, G.; Mortko, C. J.; Dang, H.; Garcia-Garibay, M. A. *J. Org. Chem.* **2004**, *69*, 1652−1662. (d) Karlen, S. D.; Ortiz, R. O.; Chapman, O. L.; Garcia-Garibay, M. A. *J. Am. Chem. Soc.* **2005**, *127*, 6554−6555. (e) Nunez, J. E.; Natarajan, A.; Khan, S. I.; Garcia-Garibay, M. A. *Org. Lett.* **2007**, *9*, 3559−3561.

(f) Godinez, C. E.; Garcia-Garibay, M. A. *Cryst. Growth. Des.* **2009**, *9*, 3124−3128. (g) Brustolon, M.; Barbon, A.; Bortolus, M.; Maniero, A. L.; Sozzani, P.; Comotti, A.; Simonutti, R. *J. Am. Chem. Soc.* **2004**, *126*, 15512−15519.

(9) (a) Dominguez, Z.; Khuong, T. -A. V.; Sanrame, C. N.; Dang, H.; Nuñez, J. E.; Garcia-Garibay, M. A. *J. Am. Chem. Soc.* **2003**, *125*, 8827−8837. (b) Horansky, R. D.; Clarke, L. I.; Price, J. C.; Khuong, T.-A. V.; Jarowski, P. D.; Garcia-Garibay, M. A. *Phys. Rev. B.* **2005**, *B72*, 0143021−0143025. (c) Rodriguez-Molina, B.; Ochoa, E. M.; Farfán, N.; Santillan, R.; Garcia-Garibay, M. A. *J. Org. Chem.* **2009**, *74*, 8554−8565.

(10) (a) Sozzani, P.; Comotti, A.; Bracco, S.; Simonutti, R. *Chem. Commun.* **2004**, 768−769. (b) Comotti, A.; Bracco, S.; Sozzani, P.; Hawxwell, S. M.; Hu, C.; Ward, M. D. *Cryst. Grow. Des.* **2009**, *9*, 2999−3002. (c) Sozzani, P.; Comotti, A.; Bracco, S.; Simonutti, R. *Angew. Chemie Int. Ed.* **2004**, *43*, 2792−2797. (d) Comotti, A.; Simonutti, R.; Catel, G.; Sozzani, P. *Chem. Mater.* **1999**, *11*, 1476−1483. (e) Schilling, F. C.; Amundson, K. R.; Sozzani, P. *Macromolecules* **1994**, *27*, 6498−6502. (f) Sozzani, P.; Bovey, F. A.; Schilling, F. C. *Macromolecules* **1989**, *22*, 4225−4230.

(11) (a) Gould, S. L.; Tranchemontagne, D.; Yaghi, O. M.; Garcia-Garibay, M. A. *J. Am. Chem. Soc.* **2008**, *130*, 3246−3247. (b) Winston, E. B.; Lowell, P. J.; Vacek, J.; Chocholoušová, J.; Michl, J.; Price, J. C. *Phys. Chem. Chem. Phys.* **2008**, *10*, 5188−5191. (c) Horike, S.; Matsuda, R.; Tanaka, D.; Matsubara, S.; Mizuno, M.; Endo, K.; Kitagawa, S. *Angew. Chem., Int. Ed.* **2006**, *45*, 7226−7230. (d) Uemura, T.; Horike, S.; Kitagawa, K.; Mizuno, M.; Endo, K.; Bracco, S.; Comotti, A.; Sozzani, P.; Nagaoka, M.; Kitagawa, S. *J. Am. Chem. Soc.* **2008**, *130*, 6781−6788.

(12) (a) Akutagawa, T.; Endo, D.; Kudo, F.; Noro, S.-I.; Takeda, S.; Cronin, L.; Nakamura, T. *Crys. Growth Des.* **2008**, *8*, 812−816. (b) Akutagawa, T.; Sato, D.; Koshinaka, H.; Aonuma, M.; Noro, S.-I.; Takeda, S.; Nakamura, T. *Inorg. Chem.* **2008**, *47*, 5951−5962. (c) Akutagawa, T.; Nakamura, T. *Dalton Trans.* **2008**, *45*, 6335−6345. (d) Kitagawa, H.; Kobori, Y.; Yamanaka, M.; Yoza, K.; Kobayashi, K. *Proc. Nat. Acad. Sci. U.S.A.* **2009**, *106*, 10444−10448.

(13) (a) Hoffmann, F.; Cornelius, M.; Morell, J.; Fröba, M. *Angew. Chem., Int. Ed.* **2006**, *45*, 3216−3251. (b) Fujita, S.; Inagaki, S. *Chem. Mater.* **2008**, *20*, 891−908. (c) Inagaki, S.; Guan, S.; Ohsuna, T.; Terasaki, O. *Nature* **2002**, *416*, 304−307. (d) Sayari, A.; Wang, W. *J. Am. Chem. Soc.* **2005**, *127*, 12194−12195. (e) Comotti, A.; Bracco, S.; Valsesia, P.; Ferretti, L.; Sozzani, P. *J. Am. Chem. Soc.* **2007**, *129*, 8566−8576. (f) Cornelius, M.; Hoffmann, F.; Fröba, M. *Chem. Mater.* **2005**, *17*, 6674−6678.

(14) Comotti, A.; Bracco, S.; Valsesia, P.; Beretta, M.; Sozzani, P. *Angew. Chem., Int. Ed.* **2010**, *49*, 1760−1764.

(15) Bracco, S.; Comotti, A.; Valsesia, P.; Chmelka, B. F.; Sozzani, P. *Chem. Commun.* **2008**, *39*, 4798−4800.

(16) Inagaki, S.; Ohtani, O.; Goto, Y.; Okamoto, K.; Ikai, M.; Yamanaka, K.; Tani, T.; Okada, T. *Angew. Chem., Int. Ed.* **2009**, *48*, 4042−4046.

(17) Pereira, F.; Valle, K.; Belleville, P.; Morin, A.; Lambert, S.; Sanchez, C. *Chem. Mater.* **2008**, *20*, 1710−1718.

(18) Kim, S. Y.; Lee, J. W.; Jung, J. H.; Kang, J. K. *Chem. Mater.* **2007**, *19*, 135−137.

(19) Jiang, D.; Yang, Q.; Yang, J.; Zhang, L.; Zhu, G.; Su, W.; Li, C. *Chem. Mater.* **2005**, *17*, 6154−6160.

(20) Peng, H.; Tang, J.; Yang, L.; Pang, J.; Ashbaugh, H. S.; Brinker, C. J.; Yang, Z.; Lu, Y. *J. Am. Chem. Soc.* **2006**, *128*, 5304−5305.

(21) Beretta, M.; Morell, J.; Sozzani, P.; Froeba, M. *Chem. Commun.* **2010**, *46*, 2495−2497.

(22) Dickson, S. E.; Crudden, C. M. *Chem. Commun.* **2010**, *46*, 2100−2102.

(23) Yamashita, H.; Roan, B. L.; Tanaka, M. *Chem. Lett.* **1990**, 2175−2176.

(24) Vold, R. L.; Hoatson, G. L. *J. Magn. Reson.* **2009**, *198*, 57−72.

(25) (a) Alcoutlabi, M.; McKenna1, G. B. *J. Phys.: Condens. Matter* **2005**, *15*, R461−R524. (b) Ellison, C. J.; Torkelson, J. M. *Nat. Mater.* **2003**, *2*, 695−700. (c) de Gennes, P. G. *Eur. Phys. J. E* **2000**, *2*, 201−203. (d) Cisternas, E. A.; Corrales, T.; del Campo, V. D.; Soza, P. A.; Volkmann, U. G.; Bai, M.; Taub, H.; Hansen, F. Y. *J. Chem. Phys.* **2009**, *131*, 1147051−1147058.

(26) (a) Schönherr, H.; Feng, C.; Shovsky, A. *Langmuir* **2003**, *19*, 10843−10851. (b) Sullivan, T. P.; Huck, W. T. S. *Eur. J. Org. Chem.* **2003**, 17−29.

(27) Conn, M. M.; Rebek, J. Jr. *Chem. Rev.* **1997**, *97*, 1647−1668.

(28) (a) Henscel, A.; Hofmann, T.; Huber, P.; Knorr, K. *Phys. Rev. E* **2007**, *75*, 0216071−0216079. (b) Huber, P.; Soprunyuk, V. P.; Knorr, K. *Phys. Rev. E* **2007**, *74*, 0316101−0316106. (c) Dosseh, G.; Xia, Y.; Alba-Simionesco, C. *J. Phys. Chem. B* **2003**, *107*, 6445−6453.

(29) (a) Huck, W. T. S. *Chem. Commun.* **2005**, 4143−4148. (b) Shao, Y.; Zerda, T. W. *J. Phys. Chem. B* **1998**, *102*, 3387−3394.

(30) Kolodziejski, W. *Chem. Rev.* **2002**, *102*, 613−628.

(31) (a) Spiess, H. W. *Colloid Polym. Sci.* **1983**, *261*, 193−209. (b) Hoatson, G. L.; Vold, R. L. *NMR Basic Princ. Prog.* **1994**, *32*, 1−67. (c) Luz, Z.; Hewitt, R. C.; Meiboom, S. *J. Chem. Phys.* **1974**, *61*, 1758−1765.

(32) Rice, D. M.; Wittebort, R. J.; Griffin, R. G.; Meirovich, E.; Stimson, E. R.; Meinwald, Y. C.; Freed, J. H.; Scheraga, H. A. *J. Am. Chem. Soc.* **1981**, *103*, 7707−7710.

(33) (a) Cholli, A. L.; Dumais, J. J.; Engel, A. K.; Jelinski, L. W. *Macromolecules* **1984**, *17*, 2399−2404. (b) Rice, D. M.; Meinwald, Y. C.; Scheraga, H. A.; Griffin, R. G. *J. Am. Chem. Soc.* **1987**, *109*, 1636−1640.

(34) (a) Schmidt, C.; Kuhn, J.; Spiess, H. W. *Prog. Colloid Polym. Sci.* **1985**, *71*, 71−76. (b) Fischer, E. W.; Hellmann, G. P.; Spiess, H. W.; Hörth, F. J.; Gearius, U.; Wehrle, M. *Makromol. Chem. Suppl.* **1985**, *12*, 189−214.

(35) (a) Pschorn, U.; Spiess, H. W.; Hisgen, B.; Ringsdorf, H. *Macromol. Chem.* **1986**, *187*, 2711−2723. (b) Geib, H.; Hisgen, B.; Pschorn, U.; Ringsdorf, H.; Spiess, H. W. *J. Am. Chem. Soc.* **1982**, *104*, 917−919.

(36) (a) Wehre, M.; Hellmann, G. P.; Spiess, H. W. *Colloid Polym. Sci.* **1987**, *265*, 815−822. (b) Simpson, J. H.; Rice, D. M.; Karasz, F. E. *J. Polym. Sci., Part B, Polym. Phys.* **1992**, *30*, 11−18.

(37) (a) Laidler, K. J. *Reaction Kinetics, Vol. 1*: Homogeneous Gas Reactions; Pergamon Press, Ltd.: Great Britain, 1963. (b) Weston, R. E.; Schwarz, H. A. *Chemical Kinetics*; Prentice-Hall, Inc.: Englewood Cliffs, NJ, 1972.

(38) Kawski, A. *Crit. Rev. Anal. Chem.* **1993**, *23*, 459−529.

(39) Ueno, Y.; Hojo, M.; Numakura, H.; Ichitsubo, T.; Saida, J. *Mater. Sci. Eng., A* **2009**, *521−522*, 232−235.

(40) We determined the energy barrier by ab initio calculations using the B3LYP/6-31G(d) method using Gaussian 03 software, Gaussian Inc, 340 Quinnipiac Street, Building 40, Wallingford, CT, 06492 Gaussian 03 Revision C.02. Frisch, M. J.; Trucks, G. W.; Schlegel, H. B.; Scuseria, G. E.; Robb, M. A.; Cheeseman, J. R.; Montgomery Jr., J. A.; Vreven, T.; Kudin, K. N.; Burant, J. C. et al. Gaussian, Inc.: Wallingford CT, 2004, Copyright © 1994−2003, Gaussian, Inc.

(41) (a) Avalue of 5.6 kcal/mol was determined for internal rotation in 1,4-divinylbenzeneusing the HF/6-31G(d) method: Hong, S. Y. *Bull. Korean Chem. Soc.* **1999**, *20*, 42−48. (b) By comparison, the related vinylbenzene (styrene)has a calculated barrier ca. 4.4 kcal/mol at the same level of theory(HF/6-31G(d)) and an experimentally observed gas-phase barrier ofapproximately 3.0−3.3 kcal/mol. Karpfen, A.; Choi, C. H.; Kertesz, M. *J. Phys. Chem. A* **1997**, *101*, 7426−7433.

(42) Jarowski, P. D.; Houk, K. N.; Garcia-Garibay, M. A. *J. Am. Chem. Soc.* **2007**, *129*, 3110−3117.

(43) Kärger, J.; Ruthven, D. M. *Diffusion in Zeolites and Other Microporous Materials*; Wiley-Interscience: New York, 1992.

(44) (a) Angell, C. A.; Ngai, K. L.; McKenna, G. B.; McMilan, P. F.; Martin, S. W. *J. Appl. Phys.* **2000**, *88*, 3113−3157. (b) Ritort, F.; Sollich, P. *Adv. Phys.* **2003**, *52*, 219−342. (c) Höchli, U. T. *Adv. Phys.* **1990**, *39*, 405−615. (d) Böhmer, R.; Ngai, K. L.; Angell, C. A.; Plazek, D. J. *J. Chem. Phys.* **1993**, *99*, 4201−4209. (e) Angell, C. A. *Proc. Natl. Acad. Sci., U.S.A.* **1995**, *92*, 6675−6682. (f) Rössler, E.; Novkov, V. N.; Sokolov, A. P. *Phase Transitions* **1997**, *63*, 201−216.

(45) (a) Roland, C. M. In *Viscoelastic Behavior of Rubbery Materials*; Oxford University Press: Oxford, 2011. (b) Ferry, J. D. in *Viscoelastic Properties of Polymers*, 3rd. ed.; Wiley: New York, 1980. (c) Poole, P. H.; Grande, T.; Angell, C. A.; McMillan, P. F. *Science* **1997**, *275*, 322−323.
(46) De Gennes, P. G.; Prost, J. In *The Physics of Liquid Crystals*; Oxford University Press: Oxford, 2010.
(47) (a) Gabel, F.; Bicout, D.; Lehnert, U.; Tehei, M.; Weik, M.; Zaccai, G. *Quarterly Rev. Biophys. 35* **2002**, *4*, 327−367. (b) Borovykh, I. V.; Gast, P.; Dzuba, S. A. *Appl. Magn. Reson.* **2007**, *31*, 159−166. (c) Ringe, D.; Petsko, G. A. *Biophys. Chem.* **2003**, *105*, 667−680.
(48) (a) Rasmussen, B. F.; Stock, A. M.; Ringe, D.; Petsko, G. A. *Nature* **1992**, *357*, 423−424. (b) Teeter, M. M.; Yamano, A.; Stec, B.; Mohanty, U. *Proc. Natl. Acad. Sci., U.S.A.* **2001**, *98*, 11242−11247.